

## Effect of N and B doping on the growth of CVD diamond (100):H(2×1) surfaces

M. Kaukonen

*Department of Physics, Technical University, FIN 02150 Helsinki, Finland*

P. K. Sitch and G. Jungnickel

*Department of Physics, Technical University, D-09107 Chemnitz, Germany*

R. M. Nieminen and Sami Pöykkö

*Department of Physics, Technical University, FIN 02150 Helsinki, Finland*

D. Porezag and Th. Frauenheim

*Department of Physics, Technical University, D-09107 Chemnitz, Germany*

(Received 29 September 1997; revised manuscript received 12 November 1997)

The doping of the chemical vapor deposition (CVD)-diamond (100):H(2×1) surface with B and N has been studied using the density-functional tight-binding method. In agreement with recent experimental results, B doping is found to lower the abstraction energies and remove diffusion barriers along the diamond growth pathway proposed by Harris and Goodwin [J. Phys. Chem. **97**, 23 (1993)]. In contrast, the Harris-Goodwin mechanism is less favorable with N doping, casting doubt on its validity in this case. We therefore propose a growth pathway on N-doped CVD diamond (100):H(2×1) surfaces. This involves a dimer opening reaction and requires less H abstraction reactions compared to the Harris-Goodwin mechanism.

[S0163-1829(98)02616-2]

### I. INTRODUCTION

The understanding of diamond growth via the chemical vapor deposition (CVD) process has proved difficult for both theorists and experimentalists alike. This is due to the large number of experimental parameters contributing to the problem and an uncertainty about the growth species. Progress has been made on the latter by the work of D'Evelyn *et al.*,<sup>1</sup> who, using isotope labeling techniques, claim to have unequivocally identified the principal growth species to be CH<sub>3</sub>. With this in mind, Harris and Goodwin<sup>2</sup> have proposed a complex mechanism for diamond growth, whose initial steps lead to the deposition of a CH<sub>2</sub> group at a bridge site above a surface reconstruction bond.

Recently, the effect of B and N doping on the CVD growth process has produced a series of intriguing results. In the case of B, various workers have found that B improves the crystalline quality of (100) CVD surfaces and enhances the *p*-type conductivity of the films.<sup>3-5</sup> Interest in the role of N in CVD diamond has been heightened by experimental observations that N preferentially catalyses growth in the (100) direction.<sup>6-8</sup> To the authors' knowledge, no serious attempts have been made to explain these phenomena theoretically. Indeed, it is unclear whether these somewhat puzzling results are compatible with the Harris-Goodwin mechanism or if in doping cases a different growth process is at work. In this paper we answer this question by investigating the effect of subsurface B and N on the energetics of the Harris-Goodwin mechanism. We find that the energies of the various growth steps are greatly altered, casting doubt on the applicability of the Harris-Goodwin method in these cases. We therefore discuss a possible alternative to the initial steps of the process.

The paper is arranged as follows. In Sec. II the theoretical tools used in this study are described. Section III explains the first few steps of the Harris-Goodwin mechanism. Section IV contains theoretical results for the N and B doping on (100):H(2×1) surfaces, while Sec. V includes a discussion of these results. Section VI proposes a model for the CVD diamond growth and a conclusion is given in Sec. VII.

### II. THEORETICAL METHOD AND THE MODEL SYSTEM

The density-functional (DF) tight-binding method (TB) derives its name from its use of self-consistent density-functional calculations for pseudoatoms in order to construct transferable tight-binding potentials for a non-self-consistent solution of the Kohn-Sham equations for the many-body case. It differs from conventional tight-binding techniques in that there is a systematic way of deriving these potentials, independent of the atom type involved. This is thus not a "parametrization" as is usually meant when one talks about TB approaches. An excellent review article written by Gorringe *et al.* summarizes the general theoretical basis of the tight-binding method and the current progress in the theory.<sup>9</sup> For an in depth description of the DF TB method, the reader is referred to Ref. 10. The DF TB method has been successfully applied to various scale carbon systems, ranging from small clusters to Buckminster fullerenes and the bulk phase,<sup>10</sup> the electronic and vibrational properties of (100) and (111) surfaces,<sup>11,12</sup> amorphous carbon systems of all densities,<sup>13</sup> as well as boron nitride<sup>14</sup> and boron and nitrogen doping of diamond and amorphous systems.<sup>15</sup> We have furthermore used the *ab initio* cluster programs of Pederson and Jackson<sup>16</sup> and Jones and Briddon<sup>17</sup> to check selected results. These programs are highly accurate but computationally very

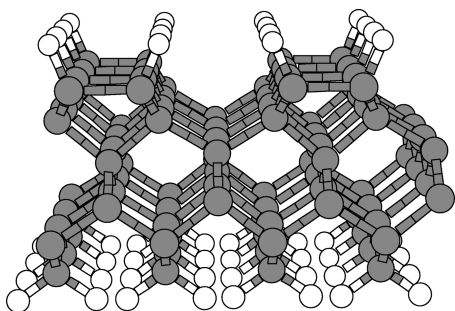


FIG. 1. Model of the reconstructed diamond (100):H(2×1) surface.

expensive; hence we are limited in these cases to very small clusters that can only represent highly idealized surfaces. Nevertheless, these calculations are useful insofar as they serve to verify the essential physics underpinning the results of our DF TB work.

The 144-atom (100):H supercell with the 2×1 reconstructed surface used in this investigation is shown in Fig. 1. It is made up of eight reconstructed surface bonds and six layers of carbon atoms. The dangling bonds on the lower surface are terminated with pseudohydrogen atoms. Unless otherwise stated, we have performed conjugate gradient relaxations, keeping the pseudohydrogen atoms and the lowest two layers of C atoms fixed. In the diffusion barrier study we have applied a constrained conjugate gradient technique (see Fig. 2).

We have observed that, owing to the relatively small size of our supercell,  $\Gamma$ -point sampling produces unphysical results. This stems from the fact that at the  $\Gamma$  point, the electronic states on the surface are lower in energy compared to the bulk states, a result that is not generally reproduced at other  $\mathbf{k}$  points. When no further  $\mathbf{k}$ -point sampling is made, this leads, in the worst cases, to extra surface charges of order half the elementary charge/atom at some of the surface atoms. This does not occur when an average over several representative  $\mathbf{k}$  points is made. The calculations have therefore been performed using the (2×2×1)  $\mathbf{k}$ -point grid recommended by Cunningham.<sup>18</sup>

The diffusing atom is moved stepwise from the starting to the final position and is allowed to relax in the plane perpendicular to the direction of the vector connecting its starting and final positions. No constraints are applied to other atoms (except the fixed lowest two layers of C atoms). The total energy of the system is recorded after each constrained conjugate gradient step giving a zero-temperature estimate for the diffusion barrier of the diffusing atom.

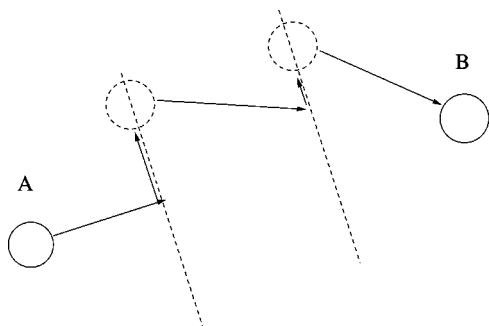


FIG. 2. Constrained conjugate gradient relaxation.

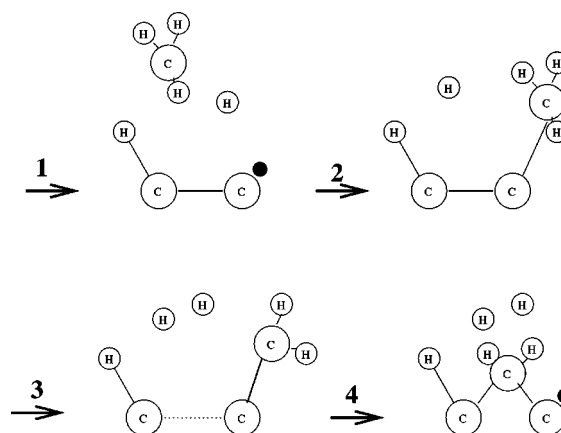


FIG. 3. Initial steps in diamond growth on the dimerized diamond (100):H surface according to Harris and Goodwin.

### III. THE HARRIS-GOODWIN MECHANISM

The initial stages of the Harris-Goodwin mechanism can be divided into four steps: (i) removal of an H atom from an otherwise fully H-terminated surface, (ii) adsorption of a CH<sub>3</sub> radical at the newly formed dangling-bond site, and (iii) loss of H from the CH<sub>3</sub> adsorbed species and simultaneous formation a C=C double bond with a surface C, which breaks its surface reconstruction bond while leaving the adjacent surface atom three-fold coordinated. It can be considered that the steps (i)–(iii) inclusive are a complex mechanism by which a CH<sub>2</sub> group is deposited in a position where it can “attack” the weakened surface reconstruction bond. This is achieved in (iv), where the CH<sub>2</sub> species rotates into the bridging position above the two surface C atoms. Steps (i)–(iv) are illustrated in Fig. 3.

We cannot accurately calculate barriers for processes of adsorption (desorption) to (from) a surface, such as those in (i)–(iii), since charge-transfer effects within DF TB mean that the detaching radical-surface complex cannot be properly represented. However, if adsorption-desorption is not accompanied by any significant electronic or structural relaxation, as indeed is the case in steps (i) and (ii) for the impurity-free surface, we can safely assume that there are no significant additional contributions to the energy barriers to such processes other than the difference in formation energy between the initial and final structures. As we shall describe in Sec. IV, this is not so for the impurity case, where structural reorganization around the N and an accompanying subsurface impurity-surface charge transfer occurs. We therefore cannot talk with any confidence about the energy barriers here. In light of this, we must limit our discussion for steps (i)–(iii), where the particle number at the surface is not conserved, to comparing formation energies for the resultant structures and making inferences where possible as to the nature of the energy barrier between. In the case of process (iv), where surface particle number is conserved, calculation of an energy barrier is possible within our method.

### IV. RESULTS

We discuss here the energetics of each of the steps of the Harris mechanism described in the preceding section for the impurity-free and the subsurface N and B calculations. We

TABLE I. Differences in formation energies for the various steps in the Harris-Goodwin procedure, plus the energy barrier for step (iv) for (i) impurity-free and (ii) subsurface N(100) surfaces.

Step Surface	Energy barrier				in (iv)
	(i)	(ii)	(iii)	(iv)	
no doping	+6.1	-5.8	+6.2	-1.0	1.7
N doping	+2.8	+1.07	-0.9	-0.5	3.0
B doping	+4.3	-4.0		-3.6	0.0

show in Table I the calculated differences in formation energies for steps (i)–(iv) inclusive and also the energy barrier for step (iv). The relative energies after each step are depicted in Fig. 4.

#### A. Step (i): Removal of H from the surface

We obtain 6.1 eV for the binding energy of a H atom to the undoped surface. This high value is in agreement with other theoretical calculations<sup>19–21</sup> and reflects the strong nature of the C—H bond. The binding energy in the presence of N, at 2.8 eV, is much lower. This is due to the occurrence of a structural relaxation after a removal of the surface H atom, consequently lowering the energy of the final structure: The N atom moves from off site to on site and an electron migrates from the impurity atom to the surface. Such a process has been described in detail in an earlier paper,<sup>22</sup> where it was shown that the position of the N atom in the lattice is governed by the Fermi level. Namely, when  $E_f$  lies at or above the single occupied  $A_1$  level associated with the defect, the N atom lowers its energy by moving offsite along one of the bonding  $\langle 111 \rangle$  directions. Conversely, if  $E_f$  is pinned below  $A_1$ , on-site N is stabilized by a charge transfer to deeper-lying states. The latter is the case here: The removal of a H atom from the surface leaves a deep-lying dangling-bond state, to which an electron migrates from the neighborhood of the N atom. We observed in Ref. 22 that this spontaneous on-site motion is accompanied by an energy gain of 1.4 eV as measured by DF TB. The

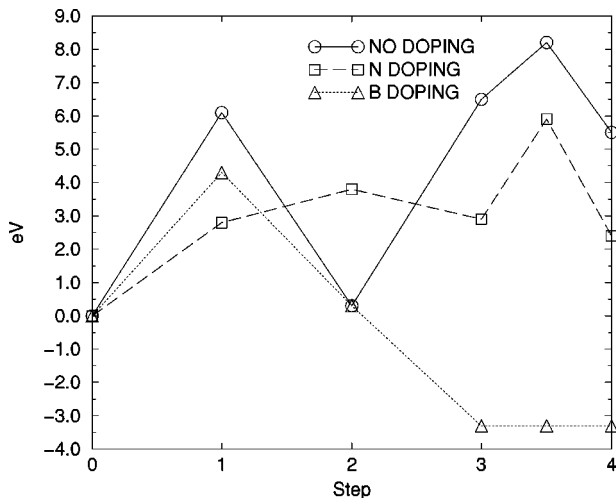


FIG. 4. Relative total energies after each step (i)–(iv). The zero of the energy is the energy of the three differently doped initial structures. The energy barrier of the step (iv) is also shown.

transference of charge to the surface is confirmed in our case by a Mulliken study, which shows that a lone pair now resides on the three-fold-coordinated surface C atom. Thus the formation energy of the resulting structure is reduced. For B doping, the binding energy is lowered to 4.3 eV. Mulliken studies show clearly that a similar charge transfer effect is also responsible here. The surface dangling-bond electron is pulled into a deep-lying subsurface acceptor state associated with the B atom.

#### B. Step (ii): Methyl absorption

The methyl radical has the largest binding energy, 5.84 eV, when attaching to the nondoped surface, indicating the strength of the  $\sigma$  C—C bond. Adsorption of the  $\text{CH}_3$  in the presence of a subsurface N atom is not favored; instead of a binding energy we find that this step costs  $\approx 1$  eV. This stems from the inherent stability of the initial structure. We also suggest that a large barrier will exist for this process since the site to which the radical should attach is no longer a dangling bond, as is the case for the impurity-free supercell, but a fully saturated lone pair. The electrostatic repulsion between the lone pair and the  $\text{CH}_3$  radical must first be overcome in order for a bond to be formed. In the B-doped case the  $\text{CH}_3$  binding energy is lowered to 4.04 eV, which again can be attributed to the charge-transfer-induced stability of the start structure.

#### C. Step (iii): H abstraction and surface rearrangement

The cost of extraction of a H atom from the  $\text{CH}_3$  species is again relatively high for the impurity free case at 6.2 eV. A C—C  $sp^2$  bond is spontaneously formed, with the C and H atoms in  $\text{CH}_2$  and the C atom on the surface all lying roughly in the same plane. The dimer-dimer bonding close to  $\text{CH}_2$  lengthens by 13%. This weakening is crucial for the final step in the growth process, in which the  $\text{CH}_2$  group rotates into a bridging position above this bond, breaking it in the process. On the N-doped surface, the  $\text{CH}_2$  fragment maintains the  $sp^3$ -like configuration, with charge transfer from the subsurface N to the  $\text{CH}_2$  adspecies, thus saturating the newly created dangling bond in the form of a lone pair [i.e., an identical charge-transfer mechanism to that of step (i)]. In contrast to the undoped case, the surface reconstruction bond is not lengthened. As we shall explain in the discussion of step (iv), this actually hinders growth. For B doping, the surface spontaneously rearranges: The  $\text{CH}_2$  group occupies the bridging position and the Harris-Goodwin cycle is completed. The energy gain in this process is 3.59 eV.

#### D. Step (iv): Migration of $\text{CH}_2$ to bridging position

We obtain an energy barrier of 1.75 eV for the  $\text{CH}_2$  diffusion to the bridge position with the undoped sample, in reasonable agreement with Mehandru and Anderson, who have found this barrier to be less than 1.92 eV.<sup>19</sup> The N-doped sample gives an energy barrier of 3.03 eV for the  $\text{CH}_2$  diffusion, which is understandable since in this case the surface reconstruction bond must be broken, which is energetically costly. For B, as previously stated, the incorporation of the  $\text{CH}_2$  fragment to the bridging position takes place with no energy barrier.

## V. DISCUSSION

### A. Nitrogen doping

It is clear from these results that the Harris-Goodwin mechanism cannot explain N catalysis of (100) diamond growth. Without doping, the hydrogen abstraction reactions (i) and (iii), as well as the energy barrier for the motion of the CH<sub>2</sub> adspecies to the bridge position (iv), are the most prohibiting steps. Our results suggest that step (ii), where in the impurity-free case a CH<sub>3</sub> group attaches to a surface dangling bond site, is severely hindered by the presence of subsurface N. Here charge transfer from N to the surface means that the CH<sub>3</sub> radical must attack a fully saturated site, where the C surface atom has an associated lone pair of electrons. The probable high-energy barrier to overcome such an electrostatic repulsion suggests that the CH<sub>3</sub> bonding to the surface in step (ii) is unlikely. Further, the subsurface-surface charge transfer severely disrupts step (iii). In the undoped case, the extraction of a H atom leads to the formation of a C=C adatom-surface *sp*<sup>2</sup> bond, together with a weakening of the adjacent surface reconstruction bond. In the doped case, charge transfer from the N atom to the C adatom saturates the dangling bond, thus leaving the C—C adatom-surface bond *sp*<sup>3</sup> like and the surface reconstruction bond unperturbed. A critical analysis of the Harris-Goodwin mechanism would suggest step (iii) to be the most crucial in the whole process since it at once places a CH<sub>2</sub> group in a position where it can attack a weakened surface reconstruction bond, subsequently forming a bridge site, which acts as a seed for further growth on the plane. This is manifestly not the case when subsurface N is present, where a full strength C—C reconstruction bond must be broken by an essentially “saturated” CH<sub>2</sub> group (the C atom having one C—C, two C—H, and an associated lone pair) rotating into the bridge site. Thus one is led to question the suitability of such a complex model in this case. In Sec. VI we describe a possible alternative.

### B. Boron doping

Although the energetics of Harris-Goodwin mechanism is perturbed by the presence of subsurface B atoms, this does not suggest that the mechanism should cease to be valid in this case. Just as for N dopants, a charge transfer is responsible for the discrepancy in the formation energies of the start and finish structures for steps (i) and (ii) between the B-doped and impurity-free structures. However, this does not lead to the problems encountered with N since charge is now transferred *from* the surface to a subsurface B acceptor level. The structure after H abstraction [step (i)] is stabilized by charge transfer, with the threefold-coordinated surface C atom now having one completely empty level. Hence, although adsorption of a CH<sub>3</sub> radical is now not as attractive as when a dangling bond is present (impurity-free surface), there is not, as is the case for N, an electrostatic repulsion preventing such an occurrence. Once the CH<sub>3</sub> group is adsorbed onto the surface [step (ii)], the rest of the Harris-Goodwin mechanism is energetically favorable. Although we cannot say exactly how big the energy barrier for H abstraction from the CH<sub>3</sub> group is, we can reason that it has as its upper bound the energy for abstraction from the undoped surface. This is due to charge transfer during abstraction:

Removal of H from the undoped surface requires the breaking of a full strength C—H bond, whereas when a B subsurface dopant is present, the energy barrier for the process may be lowered by charge transfer to the subsurface B atom. After H abstraction, the relatively electropositive CH<sub>2</sub> group is pulled spontaneously to the electron-rich bridge site. The overall energy gain in H abstraction plus CH<sub>2</sub> diffusion to the bridge site is 3.6 eV.

## VI. AN ALTERNATIVE MODEL FOR GROWTH WITH N DOPING: THE “ZIPPER” MECHANISM

We suggest a far simpler method compared to the Harris-Goodwin mechanism that would be more appropriate to describe N-catalyzed (100) growth. We have found in our studies that, although the threefold-coordinated N atom is the most stable configuration for a fully hydrogenated (100) surface, a structure where the excess “doping” charge is transferred to a surface reconstruction  $\sigma^*$  state is metastable. This has been confirmed by an *ab initio* all-electron cluster calculation, using the code developed by Pederson and Jackson,<sup>16</sup> where a difference in energy of 2.40 eV between the two structures is found. The  $\sigma^*$  state is strongly localized on one reconstruction C—C bond, which as a consequence lengthens from 1.62 Å to 2.30 Å. We have found this electron rich site to be an ideal adhesion point for a CH<sub>2</sub> species. Indeed, using the *ab initio* cluster code of Jones and Briddon,<sup>23</sup> we observe no energy barrier for the adhesion process and a binding energy of  $\approx 8$  eV. Once the CH<sub>2</sub> species adheres to the surface, the bridging and bridged C atoms are electronically saturated, thus allowing the doping charge to migrate to the next adhesion site and so on. Growth of a whole layer may thus be catalyzed by the presence of one N electron. The electron migration from the N atom to a surface dangling bond has further been confirmed by a self-consistent pseudopotential density-functional<sup>24</sup> calculation with the local-density approximation.<sup>25</sup> In this calculation the system was the same as in Fig. 1, except that one C atom was substituted with a N atom in the subsurface layer and one H atom was removed from the surface leaving a dangling bond on the surface.

We visualize the growth process in the following way: The growing crystal is a nonequilibrium thermodynamic system, in which atoms on the surface are vibrating in a variety of different phonon modes. It is perfectly plausible that the two carbons of a reconstruction bond describe a “breathing mode,” in which their C—C bond length is periodically much larger than the already weakened C—C reconstruction bond. This therefore represents an ideal target for an adhering CH<sub>2</sub> species. The energy barrier to overcome the breaking of the residual C—C reconstruction bond is further lowered by the simultaneous transfer of charge from the subsurface N to the surface. Once the CH<sub>2</sub> adhesion at the bridging site is completed, the excess electron is free to mediate a similar reaction at the adjacent site. Thus the growth of a whole layer may be catalyzed by the presence of one N electron.

Due to the geometry of the diamond structure, smooth growth in the (100) direction requires the dimer row on the upper terrace to be perpendicular to the dimer row in the lower terrace. This can be achieved by the dimer opening

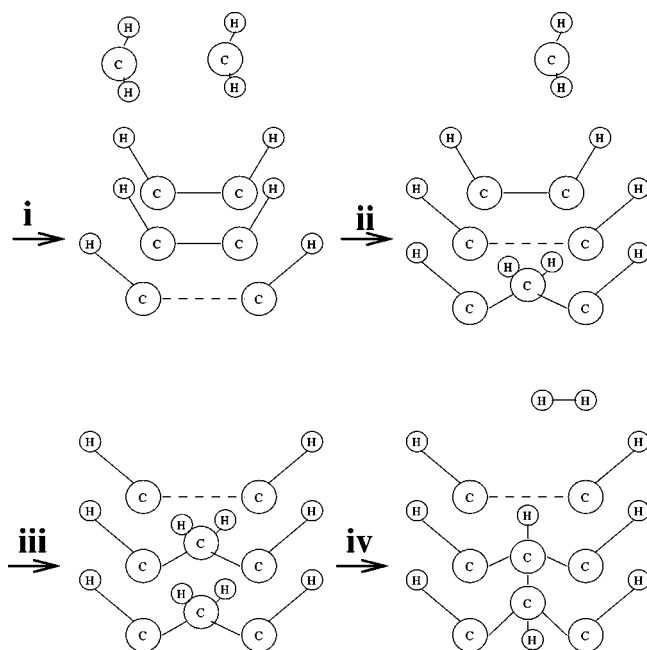


FIG. 5. Growth model with N doping of CVD (100):H diamond: the zipper mechanism. (i) The extra electron from N migrates to the surface and opens a dimer bond. (ii) A  $\text{CH}_2$  adsorbs to the open dimer and the neighboring dimer is opened. (iii) Another  $\text{CH}_2$  adsorbs to the open dimer and the next dimer is opened. (iv)  $\text{H}_2$  is abstracted and a new isolated dimer is formed to the upper terrace.

reaction if two  $\text{CH}_2$  adjacent adspecies (see Fig. 5) both eject one of their H atoms and bond together to form an isolated dimer. This isolated dimer can thereafter transform to a  $\text{C}=\text{CH}_2$  adspecies and migrate towards an existing dimer row as proposed by Skokov *et al.*<sup>26</sup> The suggested model is depicted in Fig. 5. Instead of  $\text{CH}_2$ , the  $\text{CH}_3$  molecule may also be a good candidate attaching to the open dimer. In this case two  $\text{H}_2$  abstractions are required.

In our argument thus far we have neglected two important questions. (1) How big is the energy barrier for the dimer opening? (2) Why is this method only valid for (100) orientations? We estimate (1) by noting that the essential differ-

ence between the stable threefold-coordinated N plus closed dimer structure and that of the metastable fourfold-coordinated N plus open dimer consists of the energy cost of breaking the C—C reconstruction bond and the energy gain of the on-site motion of N on losing an electron. We have calculated the former to be 2.4 eV and argue in Sec. IV above that the latter is 1.4 eV. Hence we arrive at the energy barrier of 1.0–2.4 eV, a plausible figure given the energies discussed in connection with the Harris-Goodwin mechanism.

Question (2) is answered by noting that the (100) differs from the (111) and (110) surfaces in that the clean surface possesses two dangling bonds per atom. Reconstruction and hydrogenation result in a structure where the surface C atoms have two C—C bulk bonds, one C—C surface bond, plus a saturating C—H bond. Hydrogenated (110) and (111) surfaces possess three bulk C—C bonds plus one C—H bond. The reconstruction surface (100) C—C bond, at 1.62 Å, is longer and consequently weaker and more vulnerable to attack than a bulk  $\sigma$  bond. In the case of, for example, the hydrogenated (111) surface, no such reconstruction bonds exist. To activate a surface bond would therefore require the breaking of a far stronger bulklike  $\sigma$  bond, which is then correspondingly energetically more expensive and hence less probable.

## VII. CONCLUSION

In this paper we have employed a density-functional method to investigate the effect of N and B doping on the growth of CVD diamond (100):H(2×1) surfaces. Consistent with recent CVD experiments that have shown that boron improves the crystalline quality of (100) CVD diamond surfaces, we have found the Harris-Goodwin mechanism to be an energetically favorable pathway in the CVD growth of B-doped samples. In the N-doping case, we argue that the increased diamond growth rate in the (100) direction cannot be accounted for by the Harris-Goodwin mechanism; rather we suggest an alternative model in which the (100) surface is charged by N-donor electrons. In this model a  $\text{CH}_2$  group is directly inserted into the bridging position.

<sup>1</sup>M. P. D'Evelyn, C. J. Chu, R. H. Hauge, and J. L. Margrave, *J. Appl. Phys.* **71**, 1528 (1990).

<sup>2</sup>S. J. Harris and D. G. Goodwin, *J. Phys. Chem.* **97**, 23 (1993).

<sup>3</sup>J. Mort, D. Kuhman, M. Machonkin, M. Morgan, F. Jansen, K. Okumara, Y. M. LeGrice, and R. J. Nemanich, *Appl. Phys. Lett.* **55**, 1121 (1989).

<sup>4</sup>K. Liu, B. Zhang, M. Wan, J. H. Chu, C. Johnston, and S. Roth, *Appl. Phys. Lett.* **70**, 2891 (1997).

<sup>5</sup>J. H. Won, A. Hatta, H. Yagyu, N. Jiang, Y. Mori, T. Ito, T. Sasaki, and A. Hiraki, *Appl. Phys. Lett.* **68**, 2822 (1996).

<sup>6</sup>R. Locher, C. Wild, N. Herres, D. Behr, and P. Koidl, *Appl. Phys. Lett.* **65**, 34 (1994).

<sup>7</sup>G. Z. Cao, J. J. Schermer, W. J. P. van Engkevort, W. A. L. M. Elst, and L. J. Giling, *J. Appl. Phys.* **79**, 1357 (1996).

<sup>8</sup>S. Jin and T. D. Moustakas, *Appl. Phys. Lett.* **65**, 403 (1994).

<sup>9</sup>C. M. Goringe, D. R. Bowler, and E. Hernández, *Rep. Prog. Phys.* **60**, 1447 (1997).

<sup>10</sup>D. Porezag, Th. Frauenheim, Th. Köhler, G. Seifert, and R. Kaschner, *Phys. Rev. B* **51**, 12 947 (1995).

<sup>11</sup>Th. Köhler, M. Sternberg, D. Porezag, and Th. Frauenheim, *Phys. Status Solidi A* **154**, 69 (1996).

<sup>12</sup>Th. Frauenheim, Th. Köhler, M. Sternberg, D. Porezag, and M. R. Pederson, *Thin Solid Films* **272**, 314 (1996).

<sup>13</sup>Th. Frauenheim, P. Blaudeck, U. Stephan, and G. Jungnickel, *Phys. Rev. B* **48**, 4823 (1993).

<sup>14</sup>J. Widany, Th. Frauenheim, Th. Köhler, M. Sternberg, D. Porezag, G. Jungnickel, and G. Seifert, *Phys. Rev. B* **53**, 4443 (1996).

<sup>15</sup>P. K. Sitch, Th. Köhler, G. Jungnickel, D. Porezag, and Th. Frauenheim, *Solid State Commun.* **100**, 549 (1996).

<sup>16</sup>M. R. Pederson and K. A. Jackson, *Phys. Rev. B* **43**, 7312 (1991).

<sup>17</sup>R. Jones, *Philos. Trans. R. Soc. London, Ser. A* **341**, 157 (1992).

<sup>18</sup>S. L. Cunningham, *Phys. Rev. B* **10**, 4988 (1974).

<sup>19</sup>S. P. Mehandru and A. B. Anderson, *Surf. Sci.* **248**, 369 (1991).

- <sup>20</sup>B. J. Garrison, E. J. Dawnkaski, D. Srivastava, and D. W. Brenner, *Science* **255**, 835 (1992).
- <sup>21</sup>C. D. Latham, M. I. Heggie, and R. Jones, *Diamond Relat. Mater.* **2**, 1493 (1993).
- <sup>22</sup>P. K. Sitch, G. Jungnickel, M. Kaukonen, D. Porezag, and Th. Frauenheim, *J. Appl. Phys.* (to be published).
- <sup>23</sup>R. Jones, *Philos. Trans. R. Soc. London, Ser. A* **341**, 157 (1992).
- <sup>24</sup>W. Kohn and L. J. Sham, *Phys. Rev.* **140**, A1133 (1965).
- <sup>25</sup>D. M. Ceperley and B. J. Alder, *Phys. Rev. Lett.* **45**, 566 (1980).
- <sup>26</sup>S. Skokov, B. Weiner, M. Frenklach, Th. Frauenheim, and M. Sternberg, *Phys. Rev. B* **52**, 5426 (1995).